A new method of on-line turned surface monitoring by digital image processing

Qingqun Mai[1,a], Yanming Quan[1], Peijie Liu[1] and Guo Ding[1]

[1]*School of Mechanical and Automotive Engineering, South China University of Technology, Guangzhou, China*

Abstract. A machined surface can be seen as a replica of the geometric outline of the cutting tool nose during the process of cylindrical turning, and the texture of the machined surface varies along with the tool wear. A new method of on-line turned surface monitoring is proposed in this paper by studying the grey value characteristics of the turned surface digital image. The regularity of the surface image is judged and analysed by using wavelet transform, fractal analysis, and discreteness analysis of the wavelength of the texture contour. The average wave contour, which can reflect processing state and the condition of the turned surface, is extracted from the regular texture image. Experimental results show that the turned surface condition can be monitored on-line effectively with the presented method.

1 Introduction

In automatic manufacturing, an appropriate on-line machined surface monitoring technology can effectively help to improve the production quality and efficiency. Traditionally, machined surface topography was observed by optical microscopy, scanning electron microscopy, and other methods off-line or by CCD cameras and other equipment on machine. The machined surface can be seen as a replica of the geometric outline of the cutting tool nose in cylindrical turning, and it varies along with the tool wear. Digital image processing (DIP) is an appropriate method to obtain information on the machined surface roughness and tool condition from the machined surface, which allows for on-line tool condition monitoring by combining a computer vision technique. [1]

In Ulf Persson's research, angular speckle-correlation was used in measuring surface roughness on machined surfaces, and a new technique to achieve increased repeatability by using an angle detection unit was presented[2]. Ghassan A. Al-Kindi et al. proposed a methodology to measure the surface roughness by using machine vision data. Two light reflection models (Intensity-Topography Compatible (ITC) and Light-Diffuse) were adopted and applied in this methodology[3]. S. Palani et al. presented a machine vision system, integrated with an artificial neural network, for prediction of surface roughness of end milled parts. A two dimensional Fourier transform was used to get the features of image texture in the spatial frequency domain. A back-propagation algorithm was developed, and used to train the artificial neural network. [4] Dutta, S et al. analyzed machined surface for detection of Surface roughness and tool wear, using an improvised grey level co-occurrence matrix (GLCM) technique with appropriate pixel pair spacing or offset parameter. The machined surface were imaged after cutting full length job. [5]BS Prasad et al. analyzed the surface topography image of machined surfaces during the progression of the tool wear. Their study indicated, when the tool is worn, the texture distribution strength in feed direction is weakened. With the increasing tool wear, the effect of randomly occurring deeper furrows along the feed direction on the machined surface is more apparent. [6] Narayanan M.R. et al. designed a image operator for illumination enhancement and noise filtering using evolutionary approach in the on line surface roughness measurement system in milling process. Relationship between the feature of the surface image and the actual surface roughness is obtained using regression analysis after image processing.[7] In theory, these studies paved the way for the development of an on-line and real-time machined surface-condition-monitoring system, which has not been implemented entirely yet.

Fractals have been used to analyse machined surface images for tool condition investigations. Kassim A.A et al. had investigated fractal analysis of the texture of machined surfaces. High directionality and self-affinity were dealt with by extracting the fractal features from machined surfaces images to extract tool wear information. And Hidden Markov Model is used to classify the various states of tool wear. [8] Kang M.C. et al. identified the relation between surface roughness and fractal dimension depending on coated tool wear using a generalized formula. The fractal dimension and the surface roughness showed similar tendencies depending on various cutting conditions. By obtaining images using light scattering method, the fractal dimension regularly

[a] Corresponding author: qingqmai@126.com

increases as tool wear increases. [9] It is an effective method for on line monitoring of tool wear using fractal analysis of machined surfaces. However, the algorithms above were too complex to meet the requirement of on line real-time monitoring.

A computer vision system for on-line turned surface condition monitoring is presented in this paper. Images of the turned surface from a cylindrical turning process have been grabbed and analysed. To judge whether the turning process is on the rails, wavelet transform, fractal analysis, and statistics of discreteness are applied to analyse the regularity of the turned surface texture. Then, the average wave contour is extracted from the regular turned surface texture, which is proposed as a new method for processing state monitoring in this paper.

2 Methods and theory

2.1 Machining and computer vision systems

Dry turning experiments were conducted on CNC lathe. The workpiece material was stainless steel 1Cr18Ni9Ti, and the tool material was cemented carbide K20. The turned surfaces were imaged in the process as 250×190-pixel grey-level digital images using a CCD camera (with max a frame rate of 30 fps at a full resolution of 1624×1234-pixel), a lens (with magnification of 1.0×), and a ring light source. The hardware equipment of the computer vision system for capturing cylindrical turned surface images on-line is shown in Figure 1.

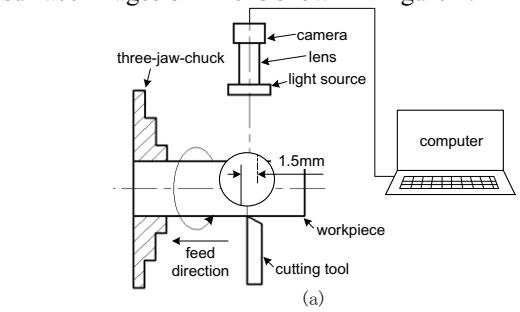

(a)

(b)

Figure 1 On-line monitoring system with computer vision for cylindrical turning

2.2 Image processing

2.2.1 Regularity of the turned surface texture

Figure 2(a) shows the image of the regular texture of the turned surface, and Figures 2(b) and (c) show images of the irregular texture of the turned surface. The significant adhesion of the turned surface is shown in Figure 2(b), and the vibratory texture is shown in Figure 2(c). As shown in Figure 2, the profiles of several rows in the turned surface image were extracted and compared. The waveform distribution of the different rows in the regular texture image was similar, but not in that of the irregular texture image.

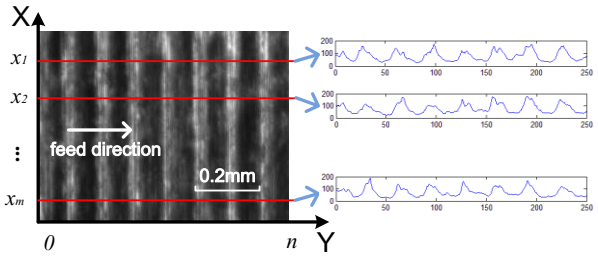

(a) Regular texture

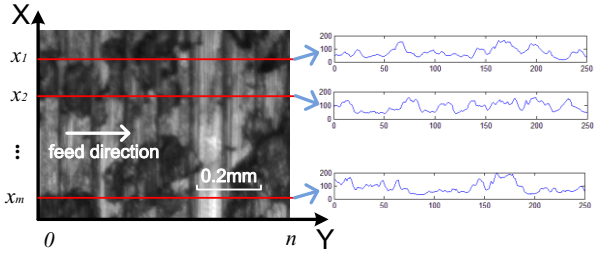

(b) Adhesive texture

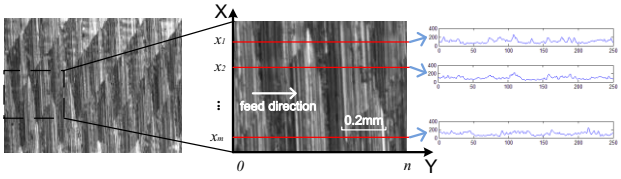

(c) Vibratory texture

Figure 2 Images of the turned surface

The regularity of the machined surface texture can be judged with the method of fractal analysis. In particular, for a cylindrical turned surface, because its texture shows parallel stripes, we can calculate the distance between two stripes as a wavelength and then analyse the discreteness of the whole wavelengths, to judge the regularity of the texture more quickly.

2.2.2 Fractal analysis of the machined surface image

Grey data were extracted from each row of the turned surface image (as shown in Figure 2) and then was calculated with wavelet transform based on the fractal theory to estimate the Hölder exponent. A series of Hölder exponents was acquired from every image. The difference between the maximum and the minimum Hölder exponent (*Ha*, Hölder amplitude) was taken as an indicator to judge the texture regularity.

The grey data vector extracted from the machined surface image was marked as x. Vector x was decomposed by wavelet transform after mirror-symmetric boundary extension. The boundary extension equation is shown as Equation 1.

$$X = \begin{cases} x_{n_m-i+1} & ,i < n_m - 1 \\ x_{-n_m+i+1} & ,n_m \le i \le n_m + n - 1 \\ x_{2n+n_m-i-1} & ,i \ge n_m + n \end{cases} \quad (1)$$

where X denotes the data after boundary extension, n indicates the length of the original data x, and n_m is the size of the mirror. The expression of the Morlet wavelet is as Equation 2.

$$\Psi(t) = \pi^{-1/4} e^{i\omega_0 t} e^{-t^2/2} \quad (2)$$

where t is an independent variable, as Y in Figure 2, and ω_0 denotes a dimensionless frequency. After the Morlet wavelet decomposition of vector X (Equation 3), the wavelet transform coefficient matrix W and analysed scales s are obtained.

$$W(s) = \langle X, \Psi_s \rangle = \frac{1}{\sqrt{s}} \int_{-\infty}^{+\infty} x(t) \Psi_s^*(t) dt \quad (3)$$

Then, the Hölder exponent was calculated:

$$W_m = max_n\, W \quad (4)$$

$$M = \frac{1}{n} \sum_{i=1}^{n} |W_{mi}|^2 \quad (5)$$

$$log_2\, M = b + a\, log_2\, s \quad (6)$$

where coefficient a is the Hölder exponent.

After calculating each Hölder exponent $a1, a2, \ldots, am$ of each row $x_1, x_2, \ldots, x_m$, respectively, in the surface image, the texture regularity indicator Ha can be obtained through Equation 7.

$$Ha = max_m\, x_i - min_m\, x_i \quad (7)$$

In a regular machined surface image, the grey curves extracted from different rows are similar, just like the fractals. Therefore, Hölder exponents show less volatility in a regular texture image than in an irregular texture image. As a result, the texture regularity indicator Ha for a regular texture will be smaller than for an irregular texture.

2.2.3 Discreteness calculation of turned surface wavelength

The contour vector x was low-pass filtered and derived to obtain the maximum points. The distance between two adjacent maximum points is defined as a wavelength; thus, a series of wavelengths (wavelength vector λ) was obtained. The discrete coefficient ξ of elements in the vector λ can be calculated using Equation 8. The texture wavelength is considered to be more uniform when the discrete coefficient ξ is smaller. Therefore, the discrete coefficient ξ of a regular texture would be smaller than that of an irregular texture obviously.

$$\xi_\lambda = \frac{\sigma_\lambda}{\bar{\lambda}} = \left(\frac{1}{n_\lambda} \sum_{i=1}^{n_\lambda} (\lambda_i - \bar{\lambda})^2 \right)^{\frac{1}{2}} / \bar{\lambda} \quad (8)$$

2.2.4 The average wave contour extracted from the regular turned surface

The regular turned surface can be seen as a collection of a large number of similar waveforms machined by the same tool nose. If the variation of tool wear during very short times can be ignored, then the waveforms machined during this period can be seen as repeated waveforms. With all repeats overlaid, the wave contour error caused by random noise will be effectively eliminated. As a result, a wave curve is obtained as the typical contour of the turned surface, which is seen as the replica of the tool nose in this moment.

3 Experiment and results analysis

3.1 Turned surface image captured on-line

The cutting parameters of the cylindrical turning of stainless steel were: Cutting speed of 100 m/min, feed of 0.1 mm/r, and cutting depth of 0.25 mm. Three cutting tools with the same material and size were used in this experiment. The geometric parameters of the turning tool were: Corner radius of 1 mm, cutting edge angle of 85°,minor cutting edge angle of 13°, rake angle of 0°, clearance angle of 14°, and minor clearance angle of 5°. The tools had different degrees of wear: Tool Ⅰ had light wear, tool Ⅱ had serious wear in the tool nose, and tool Ⅲ had obvious wear along the cutting nose and the main cutting edge. The images of the rake face contour are shown in Figure 3(a), and the tool nose morphology is shown in Figure 3(b). Cylindrical turning experiments with tools Ⅰ-Ⅲ were conducted, and the turned surfaces were imaged on-line, as shown in Figure 3(c).

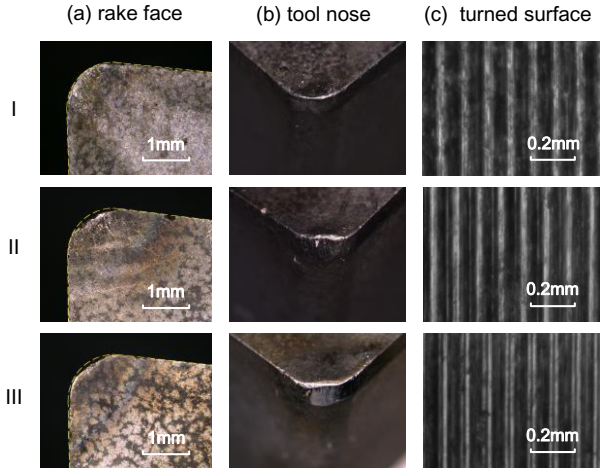

Figure 3 Images of tools and turned surfaces

3.2 Judgement of texture regularity

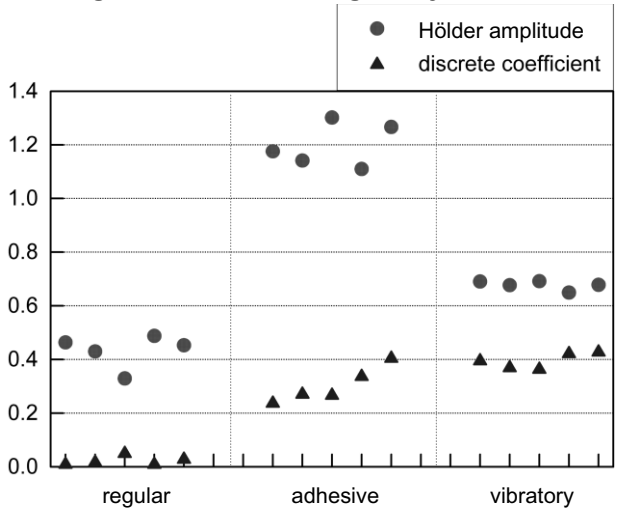

Figure 4 Judgement of image regularity

Adhesion and vibration can occur in the stainless steel machining process frequently. Adhesive texture and vibratory texture can have a serious impact on the integrity of the machined surface. The regular texture, adhesive texture, and vibratory texture were calculated for fractal and discreteness analyses. The calculated results are shown in Figure 4.

Two phenomena can be summarized from Figure 4. (1) With the illumination of the ring light, the Ha of the regular texture was smaller than that of the irregular texture, and the Ha of the adhesive texture was much greater than that of the others. (2) The discrete coefficient of the regular texture was close to 0, while the discrete coefficient of the adhesive texture was between 0.2 and 0.4, and the discrete coefficient of the vibratory texture was between 0.3 and 0.5.

Phenomenon (1) verified the principle described in Section 2.2.2. The contours extracted from the different rows from the regular machined surface image were similar, just like the fractals. However, this was not the case for the irregular machined surface image. Thus, the texture regularity indicator *Ha* of a regular texture would be smaller than that of an irregular texture. Because the texture of the adhesive surface was much more random than the vibratory texture, the vibratory texture had a greater *Ha* than the regular texture, and the adhesive texture had much a greater *Ha* than the others. The principle behind phenomenon (2) was described in Section 2.2.3. The regular texture had more uniform wavelengths and smaller discrete coefficients than the irregular texture.

To summarize, the difference in the Hölder exponent *Ha* and the discrete coefficient ξ between the regular texture and the irregular texture was obvious; thus, *Ha* and ξ can be used as indicators for the judgment of regularity of turned surface textures.

3.3 The average wave contour extracted from the turned surface image

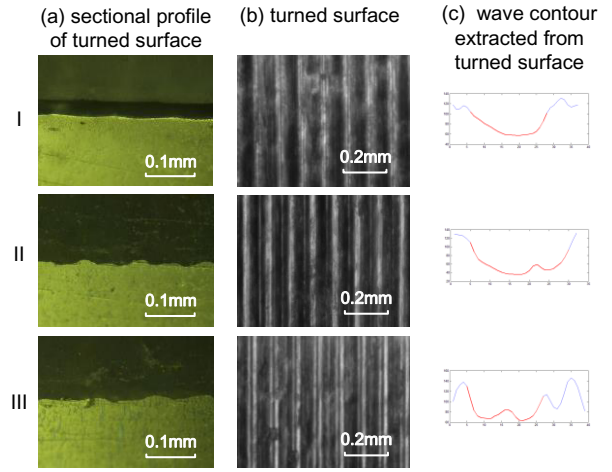

Figure 5 the average wave contour extracted from the turned surface

A small piece of sheet with a turned surface was cut down from the stainless steel workpiece with a wire-cutting method and then was buffed to view the sectional profile of the turned surface with an optical microscope, as shown in Figure 5(a). The turned surface images shown in Figure 5(b) were processed with the method described in Section 2.2.4 to extract the average wave contour (shown in Figure 5(c) in red after removing the interference). Comparing Figures 5(a) and 5(c), the average wave contour extracted from the turned surface conformed to the sectional profile of the turned surface, verifying the feasibility of extracting the average wave contour from a turned surface.

4 Conclusions

This paper concerns on-line turned surface monitoring in the cylindrical turning process. The main work and conclusions can be summarized as follows:

（1） An on-line turned surface monitoring system for cylindrical turning with computer vision and a digital image process was presented.

（2） The machined surface was analysed with fractals to judge the regularity of the surface texture and the operation of the whole machining system.

（3） For a cylindrical turning surface, the regularity of the texture can be judged simply from the wavelength discrete coefficient.

（4） The average wave contour extracted from the turned surface reflected the variety of the turned surface effectively.

（5） Turned surface condition monitoring was performed successfully with computer vision and digital image processing.

References

1. S. Dutta, S.K. Pal, S. Mukhopadhyay, R. Sen. CIRP Journal of Manufacturing Science and Technology 6, 212(2013)
2. Persson U., Journal of Materials Processing Technology, 180, 233(2006)
3. Ghassan A. Al-Kindi, Bijan Shirinzadeh. International Journal of Machine Tools & Manufacture 47, 697 (2007)
4. S. Palani, U. Natarajan. Int J Adv Manuf Technol 54,1033(2011)
5. Dutta, S., Datta, A., Chakladar, N.D., Pal, S.K., Mukhopadhyay, S., Sen, R., Precision Engineering, 36,458(2012).
6. Balla Srinivasa Prasad, M. M. M. Sarcar, B. Satish Ben. Int J Adv Manuf Technol, 55,1025(2011)
7. Narayanan M.R., Gowri S., Krishna M.M., in: Proceedings of the World Congress on Engineering 2007 (WCE, London, UK)
8. Kassim A.A., Mian Z., Mannan M.A., Machine Vision and Applications, 17, 327(2006)
9. Kang M.C., Kim J.S., Kim K.H., Surface and Coatings Technology, 193,259(2005)